Natural Resources Canada | Ressources naturelles Canada

GEOLOGICAL SURVEY OF CANADA
OPEN FILE 8808

Field data and till composition in the GEM-2 Rae Glacial Synthesis Activity field areas, Nunavut and Northwest Territories

J.E. Campbell, I. McMartin, M.W. McCurdy, P.-M. Godbout, T. Tremblay, and P.X. Normandeau

2021

Canada

GEOLOGICAL SURVEY OF CANADA
OPEN FILE 8808

Field data and till composition in the GEM-2 Rae Glacial Synthesis Activity field areas, Nunavut and Northwest Territories

J.E. Campbell[1], I. McMartin[1], M.W. McCurdy[1], P.-M. Godbout[1], T. Tremblay[2], and P.X. Normandeau[3]

[1]Geological Survey of Canada, 601 Booth Street, Ottawa, Ontario
[2]Canada-Nunavut Geoscience Office, 1106 Inuksugait Plaza, Iqaluit, Nunavut
[3]Northwest Territories Geological Survey, 4601 52nd Avenue, Yellowknife, Northwest Territories

2021

Permanent link: https://doi.org/10.4095/328454

This publication is available for free download through GEOSCAN (https://geoscan.nrcan.gc.ca/).

Recommended citation
Campbell, J.E., McMartin I., McCurdy, M.W., Godbout, P.-M., Tremblay, T., and Normandeau, P.X., 2021. Field data and till composition in the GEM-2 Rae Glacial Synthesis Activity field areas, Nunavut and Northwest Territories; Geological Survey of Canada, Open File 8808, 1 .zip file. https://doi.org/10.4095/328454

Publications in this series have not been edited; they are released as submitted by the author.

TABLE OF CONTENTS

Appendices

The Readme file provides the complete list of files and sub-directories containing the datasets:

1. Field site location and descriptions
2. Ice-flow indicator locations and descriptions
3. Sample locations and descriptions
4. Till geochemistry, <0.063 mm
5. Till matrix color and sand-silt-clay distribution
6. Till matrix carbon, LOI and carbonate contents, <0.063 mm
7. Clay mineralogy data
8. Till pebble counts, 8-30 mm, % counted
9. Gold grain and indicator mineral counts (0.25-2 mm)
10. SEM quantitative analysis
11. Metadata

List of figures

List of tables

ABSTRACT

This report releases the field datasets and analytical results from targeted surficial geology studies and till sampling completed in 2017 and 2018 in mainland Nunavut and eastern Northwest Territories as part of Natural Resources Canada's Geomapping for Energy and Minerals (GEM-2) Rae Synthesis of Glacial History and Dynamics Activity in the interior of the Keewatin Sector of the Laurentide Ice Sheet. Fieldwork consisted of targeted mapping of glacial flow indicators to resolve the relative ice-flow chronology, sampling material for geochronology to help reconstruct the glacial and post-glacial histories at a regional scale, and documenting the nature and composition of the glacial sediments in various glacial terrains. In addition to the field and analytical datasets, this report provides a detailed description of the field and analytical methods. In 2017, Quaternary geological field observations were made at 92 sites; 39 till and 16 geochronology samples were collected in 5 areas in the Baker Lake and Arviat regions, Nunavut. In 2018, the focus shifted to the Healey Lake area in eastern Northwest Territories and central mainland Kitikmeot region, Nunavut. Quaternary geological field observations were made at 72 sites; 44 till and 17 geochronology samples were collected. Till samples were analysed for matrix geochemistry and texture, gold grain counts, indicator mineral picking and probing, and pebble lithology counts.

INTRODUCTION

The Geological Survey of Canada (GSC) completed targeted surficial geology field studies and glacial sediment sampling in 2017 and 2018 as part of the GEM-2 Rae Synthesis of Glacial History and Dynamics Activity, a 3-year collaborative project between the GSC, the Canada-Nunavut Geoscience Office (CNGO) and the Northwest Territories Geological Survey (NTGS) (McMartin et al., 2017; Campbell et al., 2019). The overall goal of this Activity is to develop a comprehensive framework for the inner region of the Keewatin Sector of the Laurentide Ice Sheet (LIS) to support glacial history and dynamics reconstructions and identify distinct glacial sediment transport paths for applications to mineral exploration. The Activity's study area was divided into 2 work sectors to permit management of imagery mosaicking, database compilations and timely product deliverables. The work encompasses a compilation of glacial landforms in a two-step fashion: first in Nunavut, south of latitude 68° and east of longitude 100° (Sector 1), and then in NWT and Nunavut, south of latitude 68° and between longitudes 100° and 108° (Sector 2; Fig. 1). While data compilation and mapping of glacigenic features started in Sector 1, targeted field investigations were carried out in both Sectors to obtain data on ages of potential relict and more recent terrain surfaces, sediment composition and glacial flow directions. A new digital map of glacial geomorphic features and interpreted glacial landsystems was produced for Sector 1, covering ~415 000 km^2 in eastern Keewatin (Behnia et al., 2020; McMartin et al., 2020). The map integrates information from previous surficial geology maps and field stations with detailed mapping of glacigenic features using high-resolution ArcticDEM data and Landsat 8 imagery.

This report provides a detailed description of the field and analytical methods used during both field investigations as well as the release of the complete field datasets and analytical results from the 2017 and 2018 till sampling surveys. For a more detailed description of the separate field programs, their objectives and preliminary findings, refer to the respective Report of Activities (McMartin et al., 2017; Campbell et al., 2019). The 2017 field stations, sample description and ice-flow indicators datasets have also been incorporated in the recently published glacial geomorphology geodatabase for Sector 1 (Behnia et al., 2020).

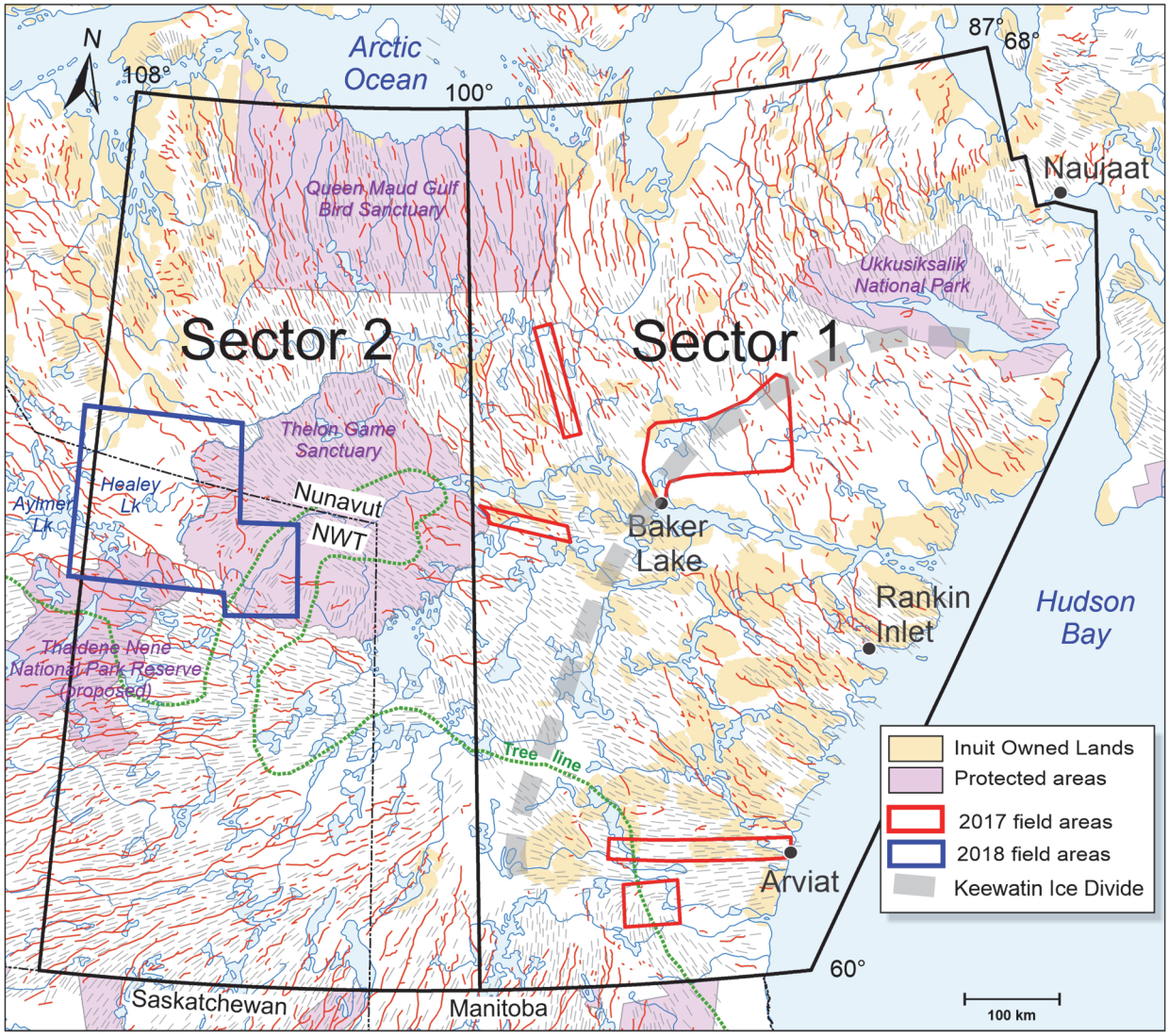

Figure 1. Region covered by the glacial compilation in central Nunavut and NWT divided into two sectors: Sector 1 and Sector 2. The five targeted field areas in 2017 are located in Sector 1 of the project compilation area (thick red). The 2018 field area is located in Sector 2 (blue). Esker trends (thin red) and glacial lineations (grey) are from Prest et al. (1968). The last approximate position of the Keewatin Ice Divide is also shown (grey dotted line). Modified from McMartin et al. (2017) and Campbell et al. (2019).

Rationale

2017 - Eastern Keewatin

The 2017 campaign was carried out in the Kivalliq region of Nunavut, centered in the Baker Lake and Arviat areas (Fig. 1). The focus of the fieldwork was to determine relative ice-flow chronology in key locations under the former Keewatin Ice Divide (KID), investigate the extent and nature of glacial landscapes under non-erosive regimes (i.e. ice divide, cold-based ice), collect glacial sediment samples to help evaluate transport characteristics in various glacial terrains, and determine marine limit position and age. As a result, five target areas were identified for field investigations (red boxes: Figs. 1, 2A and 2B).

2018 - Western Keewatin

The 2018 field campaign was carried out between Aylmer Lake and the western portion of the Thelon Game Sanctuary located in eastern Northwest Territories and central Kitikmeot region, Nunavut (Figs. 1 and 3). The glacial geology in this region is poorly understood as there has been little field-based mapping of the study area since the reconnaissance-scale mapping in the late 1950s (Craig, 1964). The focus of the fieldwork was to determine: the relative ice-flow record; glacial transport patterns; the presence and nature of relict and palimpsest terrains; the western extent of the Dubawnt Lake Ice Stream (DLIS); evidence of the McClintock Ice Divide; and the geomorphic record of the retreating ice margin.

FIELD METHODS

Field site data collection

In total, 162 ground sites and 2 remote (aerial) observation sites were visited during the 2017 (Figs. 2A and 2B) and 2018 (Fig. 3) field seasons, primarily accessed by helicopter (McMartin et al., 2017; Campbell et al., 2019). The exceptions are the sites along the Meadowbank Mine road between kilometres 0 and 5 which were accessed by truck in 2017. Sites were chosen based on previous work (glacial history models, national-scale compilations), nature of the surficial geology as observed on air photos, satellite imagery (Landsat 8) and ArcticDEM (Porter, 2018). The high-resolution 5 m digital elevation model (DEM) and Landsat imagery were used in laptop computers and portable field tablets equipped with Geographic Information System (GIS) software before, during and after field outings to identify and plan field sites accessed by helicopter, observe from the air glacial landforms identified on-screen, verify observations made from the aircraft, and help sort out field relationships measured on the ground. At each ground station work involved all or some of the following: collecting information on surface sediments (texture, colour, structure, sorting, secondary processes, etc.), landforms and small-scale erosional features on bedrock, measuring the elevation of the post-glacial marine limit (2017), till sampling, and sampling materials for age dating. The terrain, ice-flow indicators, dughole and sample media were photographed at each field site. Site data were digitally captured in the GANFELD system using a GIS-based tablet. Altitude measurements of the dating sampling sites and the post-glacial marine limit features were collected with a handheld GPS unit. In 2017, a barometer altimeter calibrated to benchmarks using a Track-It™ Barometric/Temperature Data Logger was also used to collect the altitude measurements (see method in Randour et al., 2016). The descriptions of the field sites are provided in Appendix 1.

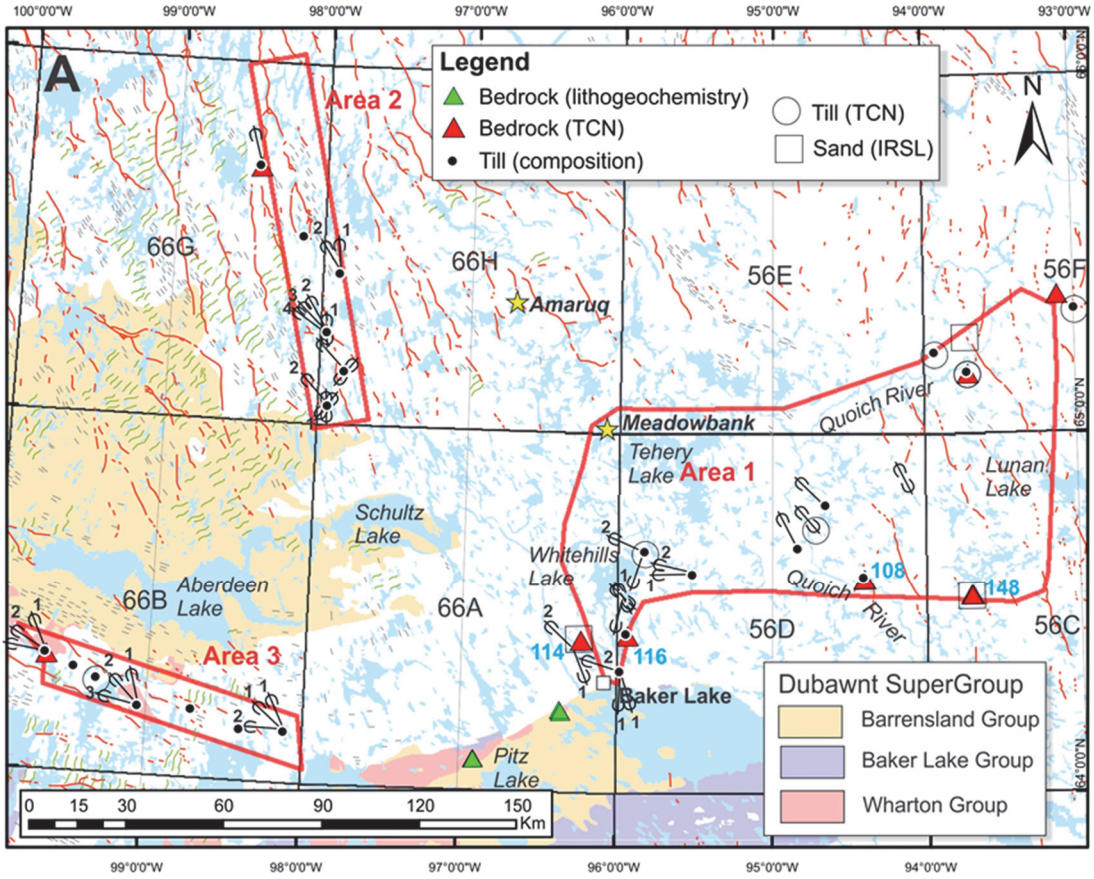
A
Legend
Bedrock (lithogeochemistry)
Bedrock (TCN)
Till (composition)
Till (TCN)
Sand (IRSL)
N
Area 2
66G
66H
Amaruq
56E
56F
Meadowbank
Quoich River
Tehery Lake
Area 1
Lunan Lake
Schultz Lake
Whitehills Lake
66B
Aberdeen Lake
66A
108
148
56D
56C
Area 3
114
116
Baker Lake
Dubawnt SuperGroup
Barrensland Group
Baker Lake Group
Wharton Group
Pitz Lake
0 15 30 60 90 120 150 Km

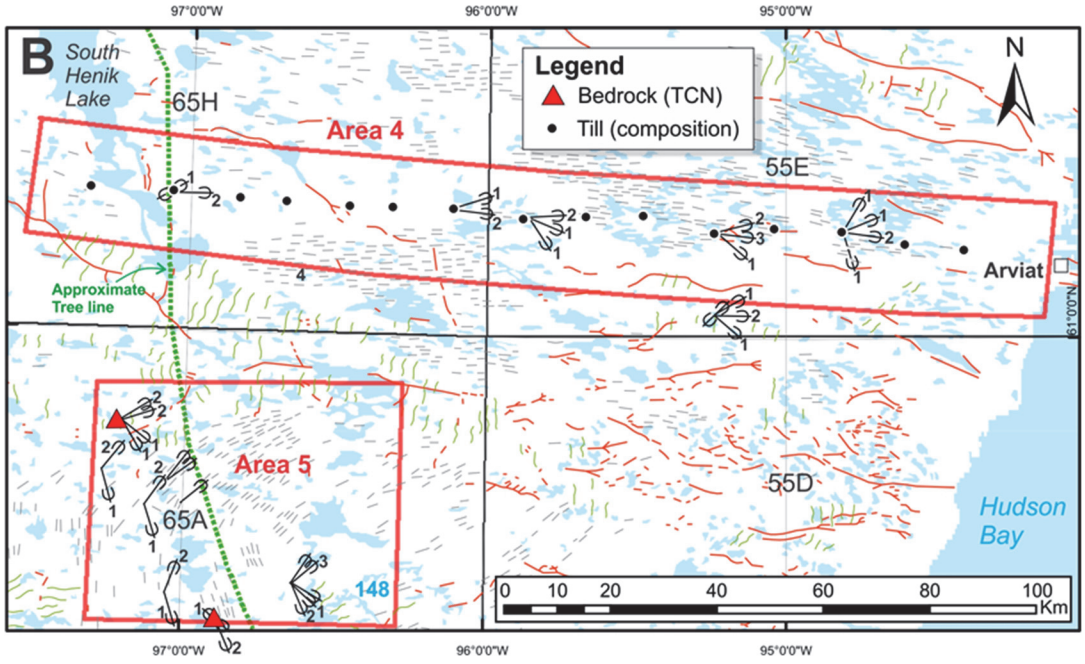
B
South Henik Lake
65H
Area 4
Legend
Bedrock (TCN)
Till (composition)
N
55E
Approximate Tree line
Arviat
Area 5
65A
55D
Hudson Bay
148
0 10 20 40 60 80 100 Km

Figure 2. *Location of samples and striations collected in 2017.* ***A)*** *Areas 1, 2 and 3.* ***B)*** *Areas 4 and 5. Where determined, the relative ages of striations are shown; marine limit elevations (m asl) are indicated (text in blue). Eskers (red), glacial lineations (grey) and transverse landforms (green) are from Aylsworth and Shilts (1989). Generalized extent of Dubawnt Supergroup lithologies are from Paul et al. (2002). Yellow stars indicate Agnico Eagle Mines projects north of Baker Lake. Figure from McMartin et al. (2017).*

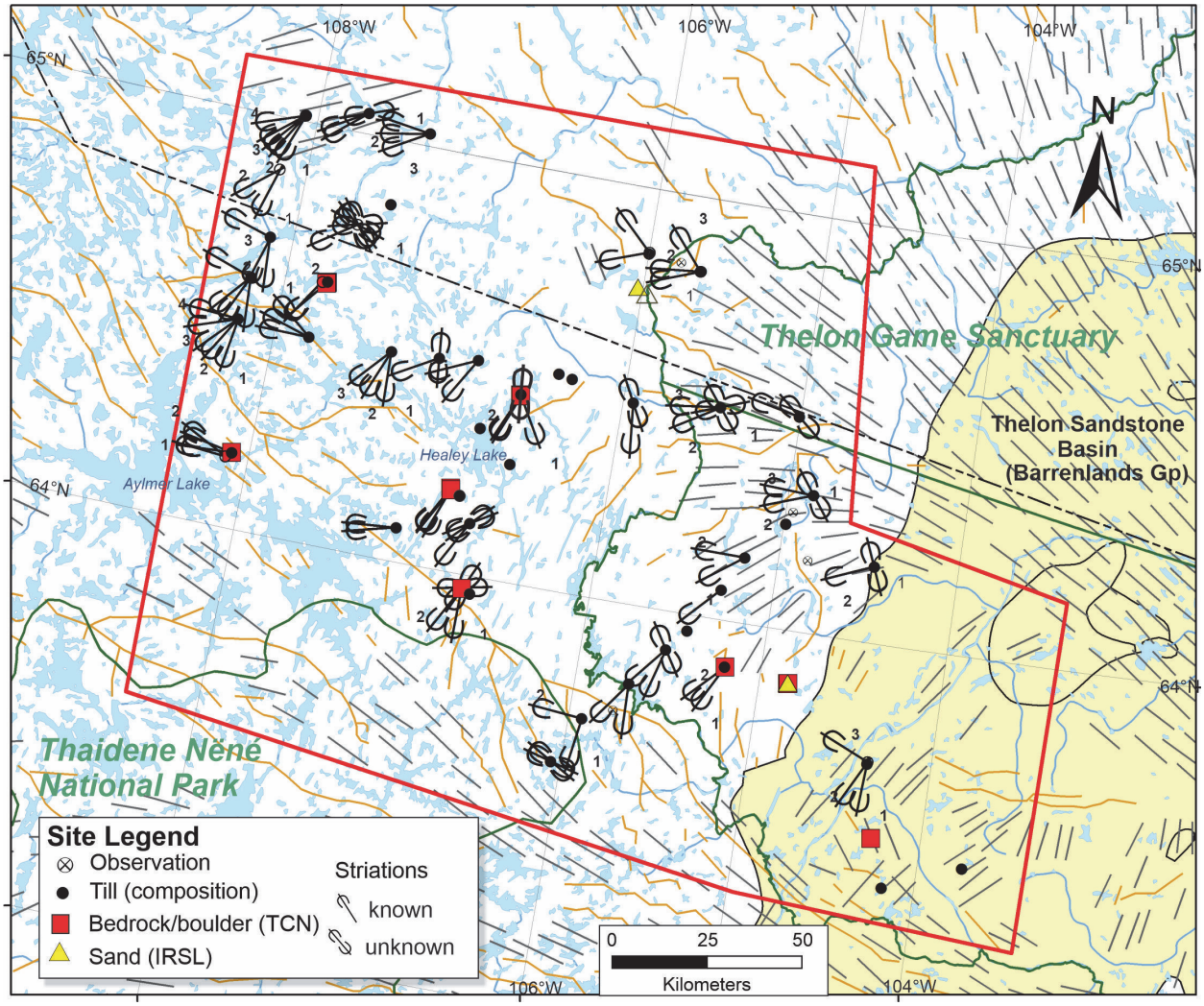

Figure 3. Location of field stations, samples and striations collected in 2018. The relative ages of striations are shown. Eskers (orange) and glacial lineations (grey) are from Prest et al., (1968). Thelon Basin outline is from Harrison et al. (2011). Figure from Campbell et al., (2019).

Ice-flow Indicator Mapping

Indications of ice flow directions are determined from the orientation and sense of both streamlined landforms (e.g. drumlinoid features and crag-and-tails) and small-scale erosional indicators (e.g. striations, chattermarks, crescentic gouges, roches moutonnées; Fig. 4). In total, 184 small-scale erosional indicators were measured at 74 sites (2017 – 86 measurements at 34 sites; 2018 – 97 measurements at 40 sites; Figs. 2 and 3). The relative ages of ice flows were established for multiple indicators at 50 sites (e.g. Fig 4A) as well as where cross-cutting landforms (Fig.4B) were observed on the imagery and in the field. Small-scale ice-flow indicator locations, descriptions and measurements are provided in Appendix 2.

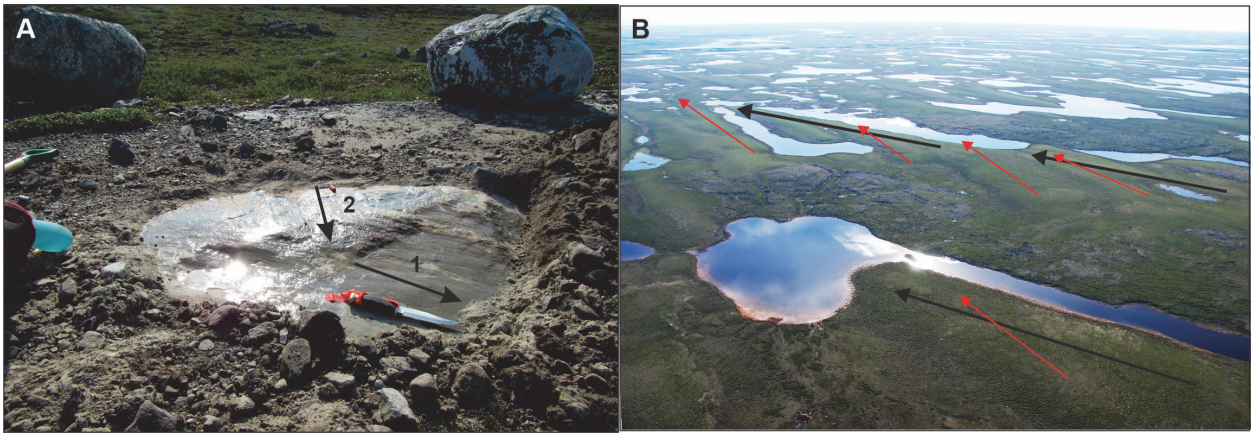

*Figure 4. **A**) Multiple sets of striations at site 18CBB-C034 (Appendix 2) indicate relative age of two ice-flow phases. Striae preserved on a protected lee surface (1) records older flow to the SW (232°). Striations on top of the outcrop (2) record the younger, main ice flow to the WNW (285°). **B**) Palimpsest terrain: smaller, younger WSW trending drumlins overprint older south trending streamlined features (Photos by J. Campbell, NRCan photos A) 2021-118 and B)2021-119; Campbell et al., 2019).*

Till and bedrock sampling

Till samples were collected from a variety of glacial terrain types to characterize the sediments associated with these terrains (i.e. relict, ice divide, ice streams, veneers, plains and modified), and to determine their composition and provenance to support regional transport-dispersal studies. A total of 85 till samples were collected during the two field campaigns, specifically 41 in 2017 and 44 in 2018.

In 2017, 39 small and large till samples were collected from 38 sites to characterize the regional glacial transport under various settings (Figs. 2A and 2B). Ten samples were collected from northeast of Baker Lake in Area 1 over the KID, six samples along an 80 km-long north-northwest transect north of the Thelon Basin in Area 2, eight samples along 80 km of the Dubawnt Lake Ice Stream (DLIS) in Area 3, and fifteen samples along 160 km of the Maguse Lake Ice Stream (MLIS) in Area 4. In addition to the regional samples, 2 small till samples were collected at 2 sites for a total of 41 samples for geochemical analysis. Separate till samples were collected at six sites to estimate the amount of glacial erosion and to be used as a proxy for estimating the changes in relative basal thermal regime by terrestrial cosmogenic nuclide (TCN) exposure dating (e.g. Staiger et al., 2006) (Fig. 2A).

In 2018, 42 large and small till samples were collected from 40 sites plus 2 small samples from 2 additional sites, all of which were taken from a variety of glacial terrains, namely relict (cold-based), warm-based deglacial, palimpsest and the DLIS. Five of the samples were collected from greenstone bedrock regions to obtain regional background elemental concentration and test for mineral prospectivity. Samples were also collected along two transects, to test regional glacial transport of debris from the Thelon sandstone basin and to complement other transects completed in the Keewatin region of Nunavut and NWT (i.e. Kjarsgaard et al. 2014; McMartin, 2000, 2017; McMartin et al., 2013, 2015, 2017, 2019; Campbell et al., 2016, 2017, 2020) (Fig. 3).

During both years, the till samples were collected from flat till surfaces in Cy- or C-horizon material from hand dug pits primarily in frost boils, at an average depth of 38 cm (2017) and 60 cm (2018) (Fig. 5A and B). Sample holes were dug in both inactive and active (fresh) frost boils depending on availability. In western Keewatin, the permafrost is more discontinuous and the frost boils were commonly inactive resulting in deeper oxidation. At each site, one small sample (~3 kg) and one large sample (mean=12.1 kg;

range=9.3-15.1 kg) were collected in plastic bags (Fig. 5B). Field duplicate samples between 5-10 m away from the original sample hole were collected at three regional sites (2017=1; 2018=2). The samples were submitted for compositional (textural, geochemical and clast lithology), indicator mineral and precious metals grain analyses. Sample collection and analyses were conducted following GSC protocols (McClenaghan et al., 2020). Till sample locations and descriptions are provided in Appendix 3.

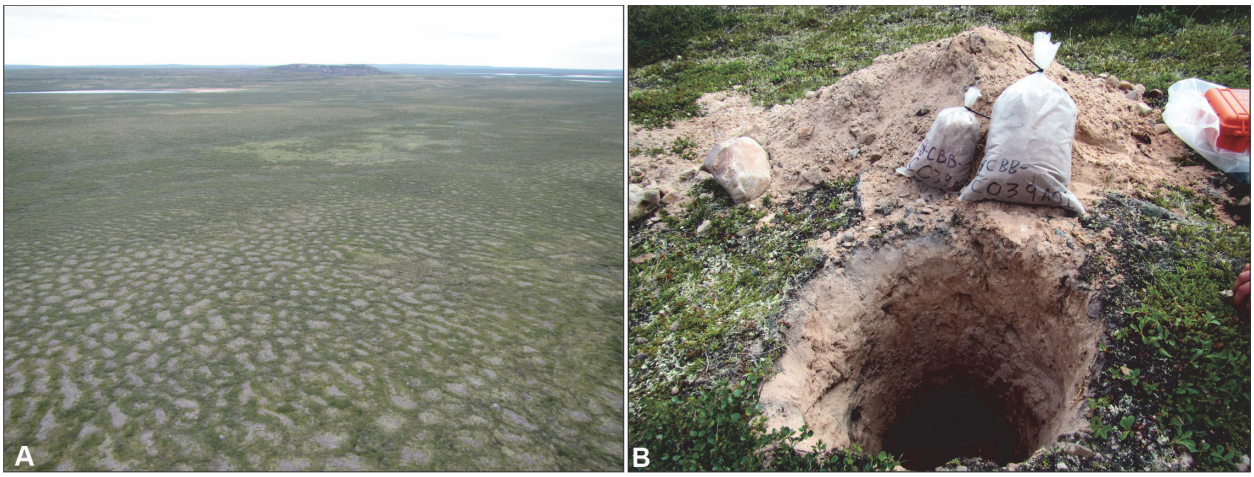

Figure 5. ***)*** *Samples were primarily collected from frost boils such as from the Dubawnt-rich pink-colored till within the DLIS in Area 3, Sector 1. Photo by I. McMartin, NRCan photo 2021-121 (McMartin et al., 2017).* ***B)*** *Large (~12 kg) and small (~3 kg) till samples are collected mainly from the C-Cy soil horizon in hand dug pits (18CBB-C039A01). Photo by J. Campbell, NRCan photo 2021-120 (Campbell et al., 2019).*

Five bedrock samples from the Dubawnt Supergroup lithologies (e.g. Rainbird et al., 2003) were collected for whole-rock geochemical analysis to determine the geochemical signature of these distinctive lithologies in till. Four representative samples were collected from the Baker Lake Basin in 2017: 1) quartz-sandstone from the Thelon Formation (Barrensland Group), 2) red sandstone from the Amarook Formation (Wharton Group), 3) rhyolite from the Pitz Formation (Wharton Group), and 4) ultrapotassic lava flows from the Christopher Island Formation (Baker Lake Group). An additional sample of the Thelon Formation sandstone was collected south of the Thelon River, western Keewatin, in 2018. The lithogeochemical results are not included in this report.

Geochronological Sampling

The inner region of the Keewatin Sector of the LIS has limited chronological constraints on its deglacial history (see Dalton et al. 2020). It also contains potential relict terrains where surfaces were preserved under non-erosive basal ice regimes (cold–based) during the last glaciation (see McMartin et al., 2017, 2020; Campbell et al., 2019). The coastal regions were affected by post-glacial marine inundation but the age of the marine limit is poorly constrained (Randour et al., 2016). Therefore geochronological samples were collected for three purposes: 1) to provide absolute ages to help establish a minimum age for ice-free conditions and improve the chronology of ice margin retreat; 2) test the relative inheritance or estimate the amount of glacial erosion; and 3) constrain the timing of marine emergence along the coast of Hudson Bay in eastern Keewatin (Sector 1). Two dating methods were employed; TCN surface exposure dating and infrared stimulated luminescence (IRSL) dating.

Thirteen bedrock samples were collected from 10 sites (Fig. 2) in various settings for TCN dating in 2017 and fourteen bedrock/boulder samples were collected from eight sites in 2018 (Fig. 3). The lithologies collected were granitoid, quartz-veins or quartz-rich metasediments in composition to ensure

sufficient quartz mineral grains for ^{10}Be and/or ^{26}Al exposure age dating (Gosse and Phillips, 2001). Selected samples were analysed at the Cosmogenic Isotopic Science laboratory at Dalhousie University.

As a complement to TCN dating, samples were collected for IRSL dating. This method determines the depositional age of detritic feldspar grains in sediment after they have been 'zeroed' (e.g. by exposure to sunlight during transport) before burial (Huntley and Lian, 1999; Lamothe, 2016). In 2017, a total of three IRSL samples were collected in sites reflecting minimum deglaciation chronology and sites standing directly at the marine limit (Bateman, 2015). For the 2018 campaign, two IRSL samples were collected from well-sorted fine- to medium-grained sands in raised beaches developed on glaciolacustrine ice-contact deltas. The IRSL ages will help constrain the timing of the pro-glacial lake(s) stands at ice margins and provide minimum ages for the ice margin retreat. The IRSL samples were analysed at the Laboratoire de luminescence (LUX) at Université du Québec à Montréal.

More detailed discussions concerning the geochronology sampling are provided for the respective years by McMartin et al. (2017) and Campbell et al. (2019). Detailed description of the TCN and IRSL sites, sampled material, sampling methods and the resulting dates will be released in a subsequent publication.

ANALYTICAL PROCEDURES AND QA/QC RESULTS

Till sample preparation

Sample preparation and analytical procedures for all till samples are summarized below in Figure 6. The samples were prepared at the GSC Sedimentology Laboratory following procedures described by Girard et al. (2004) and outlined in the GSC protocols (e.g. McClenaghan et al., 2020). A split of approximately 2 kg was taken from the small (~3 kg) till samples and were air-dried and dry-sieved, using a stainless steel 230 mesh screen to obtain the <0.063mm (silt+ clay) fraction for geochemical analyses. A second split of the samples was taken for colour, texture and clay mineralogy (2017) analyses. Description of sample preparation for each analyses is discussed under the respective sections below. Approximately 800 g of the original 3 kg samples and the excess <0.063 mm material not used for geochemical analyses are archived at the GSC.

In total, 82 large (~12 kg) till samples, including 1 lab duplicate, and 4 blanks were shipped to Overburden Drilling Management Ltd (ODM), Ottawa for processing, production of heavy mineral concentrates and picking of precious metal grains and indicator minerals following protocols laid out by Plouffe et al. (2013a, b). Samples were disaggregated in water and sieved at 2 mm to remove all clasts and produce the <2 mm size fraction material for heavy mineral concentrate processing. The >2 mm sample fraction was further wet-sieved to collect the 8-30 mm clast fraction for lithological analysis. Description of the heavy mineral processing and mineral picking is provided under the **Heavy mineral processing, Au grains and indicator mineral picking** section below.

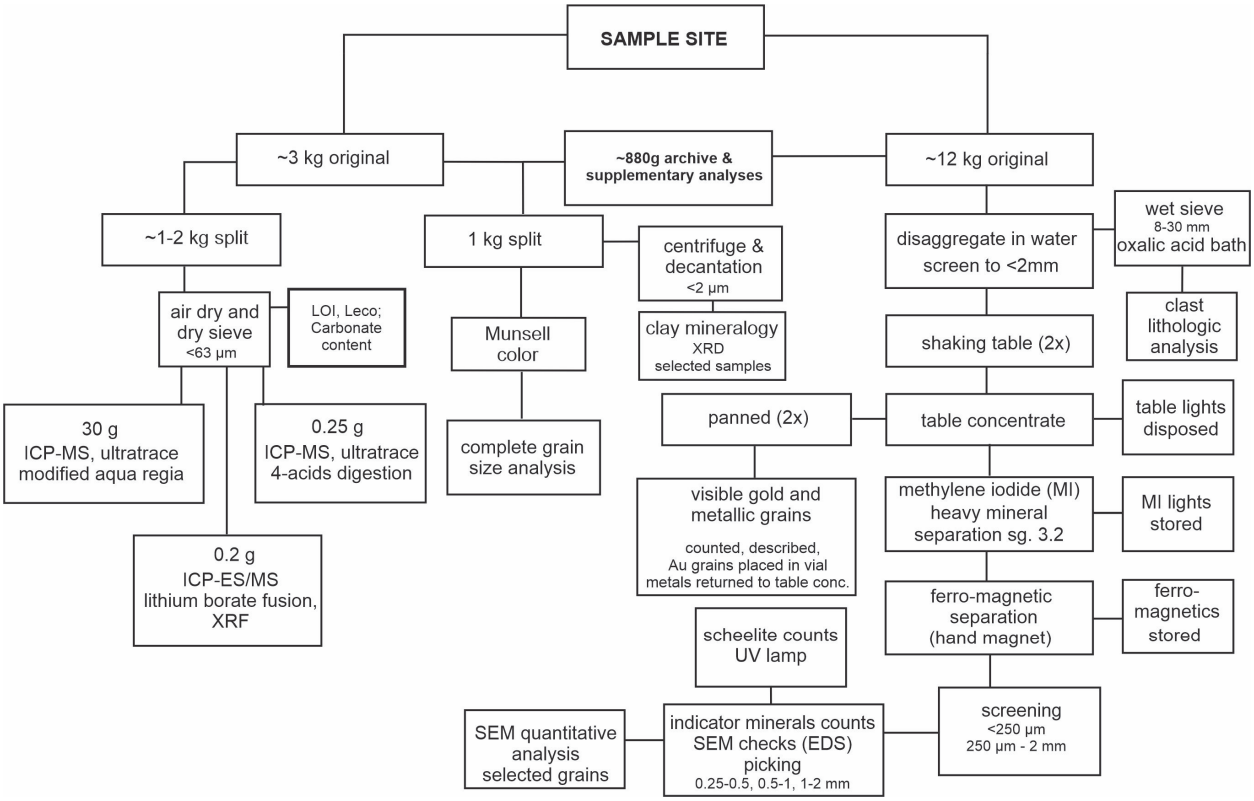

Figure 6. Flow sheet showing steps in till sample processing (modified from McMartin et al., 2019).

Till matrix geochemistry (<0.063 mm fraction)

In total, 85 till samples were submitted for geochemical analyses of the <0.063 mm size fraction. The till geochemistry package used in this study is similar to McMartin el al. (2019) and Campbell et al. (2020) to ensure comparable results and regional data continuity, the only analytical difference between the years is the major oxides (see below). Both the 2017 and 2018 till samples were analyzed at Bureau Veritas Minerals (BVM). The following lists the types of analyses done by year (Bureau Veritas, 2021):

2017

MA250 – Multi-acid/ultra-trace ICP-ES/MS, 59 elements (0.25 g)
AQ252-EXT + REE – *Aqua regia* ICP-ES/MS, 53 + 12 elements (30 g)
LF100 – Lithium borate fusion ICP-MS, refractory and REEs, 31 elements (0.25 g)
XF700 – X-ray fluorescence, 11 whole rock major oxides + Loss on Ignition (LOI), Ba, Sr, SO_3

2018

MA250 – Multi-acid/ultra-trace ICP-ES/MS, 59 elements (0.25 g)
AQ252-EXT – *Aqua regia* ICP-ES/MS, 53 elements (30 g)
LF200 – [(LF100 Lithium borate fusion ICP-MS+ LF302-EXT (11 major oxides ICP-ES, 34 elements + Ce, Co, Cu, Zn, LOI) + TC000 (total C & S)] (0.25 g)

Analysis was conducted on a 0.25 g aliquot of the <63 µm fraction of the till matrix by ICP-MS

after a four-acid digestion (HNO_3-$HClO_4$-HF dissolved in HCl: Group MA250: 59 elements). An additional 30 g aliquot of the <63 µm fraction of each till sample was also analysed for a suite of trace, major and rare earth elements (2018) using a modified *aqua regia* digestion (HCl-HNO_3, 1:1, 95°C) followed by ultratrace ICP-MS with an extended package for Pt and Pd (Group AQ252-EXT: 53 elements).

In 2017, a total whole rock characterization of the till sample was carried out by X-ray fluorescence analysis (XF700). Dried samples were mixed with lithium tetraborate/metaborate flux followed by fusion and casting into glass beads (Bureau Veritas, 2021). In 2018, whole rock characterization was done by lithium tetraborate/metaborate fusion/ ICP-MS. A 0.25 g aliquot was analysed for oxides plus Cu, Mo, Ni, Pb, Sc and Zn by ICP-ES and for trace elements by ICP-MS following a lithium metaborate/tetraborate fusion and dilute nitric acid digestion (LF200:49 elements + LOI). Total carbon and sulphur were analysed by LECO (> 1350° C) as part of the same package (TC003).

Although, as noted above, the till geochemistry package used in 2018 differs from that used in 2017, the multi-acid package (MA250) was used both years and the aqua regia package with a 30 g aliquot (AQ252) was the same except for the additional REE extension (Pr, Nd, Sm, Eu, Gd, Tb, Dy, Ho, Er, Tm, Yb, Lu) added in 2018. A lithium metaborate fusion was used both years (LF100; 31 elements) but an additional whole rock characterization extension that includes major oxides (LF200), additional elements (Ce, Co, Cu, Zn, LOI) and total C and S (TC100) was requested in 2018. With the exception of Mo, Cu, Pb, Zn, Ni, and Sc (LF), SO3, Sr and Ba (XF), Cr2O3 (XF/LF), Total C and S (LECO), and partial analysis of REE by aqua regia (Pr, Nd, Sm, Eu, Gd, Tb, Dy, Ho, Er, Tm, Yb, Lu), most elements have comparable equivalents between 2017 and 2018. These results can be classified as total (XRF), near-total (LF, MA) and partial (AQ) although both near-total and total can in fact produce 'total' data (McCurdy and Garrett, 2016).

Loss-on-ignition (BVM Code TG001) was determined in 2017 and 2018 using a 1 g sample. Each sample was placed in a crucible, weighed and ignited to 1000° C for one hour in a muffle furnace. The oven was then cooled to 100º C and the crucibles transferred to a desiccator followed by cooling to room temperature. The crucibles were weighed again to determine the loss-on-ignition. The lower limit of detection is indicated as -5.1% to allow for reporting of negative loss on ignition results. Negative LOI results may occur in some samples where a weight gain occurs during ignition, generally due to the oxidation of iron minerals (Bureau Veritas Minerals, 2021).

Total carbon and sulphur (TOT/C and TOT/S; BVM Code TC000-C & -S) were determined in 2018 by igniting 0.1 g of <63 µm sample with a flux in an induction furnace. Released carbon was measured by adsorption in an infrared spectrometric cell. Results are total and attributed to the presence of carbon and sulphur in all forms (Bureau Veritas Minerals, 2021).

Detection limits, raw analytical data and data exportable into GIS formats (less than detection limit. values= ½ d.l.) are given in Appendix 4. For the GIS formatted data in Appendix 4, the order of the elements is the same as the lab reports for each year and the number following the element refers to the analytical method (e.g. Cu_3_ppm) as summarized below in Table 1. The metadata for the till matrix geochemical analyses are summarized in Appendix 11.

Method no.	2017	2018
1	MA250	MA250
2	AQ252	AQ252
3	LF100	LF200
4	XRF	
5		TC000-C & -S

Table 1. List of analytical methods and the associated annotated number used in 2017 and 2018

Quality Accuracy and Quality Control (QA/QC)

Accuracy and precision of analytical data returned from commercial laboratories were determined by including analytical duplicates, primary standards (control reference materials: Till-4) and silica blanks (qtz-133256) within the three sample batches submitted to the analytical laboratory in 2017 and 2018. Analysis of laboratory duplicate samples was used to monitor analytical precision of the geochemical results. Four analytical duplicates were prepared during sample preparation (see Appendices 4 and 4A). Normally, the duplicates are prepared from field duplicate samples and given a new sample number. In 2018 this was the case (e.g. 18CBB-C034A02 and lab duplicate 18CBB-C002C01) however, in 2017 there was not enough material to use the field duplicate therefore two routine samples were selected and were labelled with a similar sample code (e.g. 17MOB070A01 and lab duplicate17MOB070B02). Analytical duplicates were inserted at the beginning of each batch and about every 20-25 samples. Analysis of primary standards was used to monitor analytical accuracy of the geochemical results and the standards were inserted randomly within each block of ~20 samples. To monitor potential cross-contamination during the sieving process and to purge the sieves between sample batches, silicic acid blanks were sieved at the beginning of each block of about 20 samples and submitted as part of the sample batch for geochemical analysis. The QA/QC statistics results discussed below are included in Appendix 4A, Tables A4a-1 to A4a-9.

Accuracy

Results from the analysis of Till-4 were divided into three groups based on the approximate degree of determination of concentration, partial (*aqua regia*), near-total (multi-acid), and total (XRF and lithium borate fusion. For statistical purposes, multi-acid data for two aliquots of Till-4 from 2017 and two aliquots from 2018 were grouped for univariate statistical analysis (Mean, Standard Deviation - SD and Relative Standard Deviation - RSD). *Aqua regia* (AQ) results from both years were grouped together and REE data from 2018 were included in Table A4-1. 'Total' data for oxides (XRF and LF), with the exception of Cr_2O_3 (2017), Cr_2O_3 (2018) and SO_3 (2017) were grouped together from both years in Table A4a-2, and multi-acid (MA) data are listed in Table A4a-3.

No RSD % is calculated for the elements with concentrations below detection limits in TILL-4, including Pd (AQ), Ta (AQ), Pt (AQ) Ge (AQ), Ni (LF) and Re (MA). For *aqua regia*, caution should be observed for results of Be, Hf, Re, Hg, B, and Se at low concentrations. One element in TILL-4, W, has a concentration exceeding both the upper detection limit of 100 ppm (AQ) and 200 ppm (MA) and consequently no RSD is calculated. A combination of relatively high RSD values (>20%) and low mean concentrations in TILL-4 for elements such as Be (LF) and Se (MA) may be the result of elemental concentrations held within discrete, often refractory, minerals, including spinels, beryl, tourmalines, chromite, zircon, monazite, niobates, tungstates, topaz, tantalite and cassiterite (Crock and Lamothe, 2011).

Accepted values for total analysis of TILL-4 for Cr_2O_3 by XF and LF are not available, but data from XRF results in 2017 suggest that precision may be unreliable at concentrations close to the limit of detection. Results from Sr and Ba by XF have an RSD greater than 20%, but as these results are based on only two samples, the RSD may improve with more samples.

Precision

Precision was estimated from data for four analytical duplicate pair, two in 2017 and two in 2018. Based on an acceptable limit of ±10% RSD, Au and B by AQ, Be and Mo (LF) and Cr_2O_3 (XF) should be treated with caution at concentrations close to the limits of detection (see below). Multi-acid digestion for Be, Ag, Cd, W, In, Te, Tb, and Tm fall outside the ± 10% RSD limits.

Since there is an established relationship between concentration and precision (Thompson & Howarth, 1978), relatively poor precision is predicted at concentrations near the lower determination limit but improves as concentrations increase to an optimum level for the instrument being used, and then falls off at the upper limit of concentration that the instrument is capable of measuring (Fletcher, 1981). The values listed under Precision % (RSD %) in Tables A4a-4, A4a-5 and A4a-6 thus provide a measure of the average precision over the ranges of concentrations provided in the table. Because of the small sample size (four duplicates) these values are themselves imprecise, however they may suggest where caution is warranted.

Comparing Analytical Methods

The sample groups are relatively small, 41 samples in 2017 and 44 samples in 2018. There are two certified reference standards in each group (TILL-4) along with one field duplicate for 2017 and two field duplicates for 2018. There are two lab duplicate pairs in the 2017 set and two lab duplicate pairs in 2018. Finally, there are three silica blanks inserted in 2017 samples and two blanks in 2018 samples.

Partial, Near-Total and Total Analytical Results

A majority of the chemical analyses returned to the GSC from commercial and government labs fall into three broad categories; ‘partial’, ‘near-total‘ and ‘total’ (McCurdy and Garrett, 2016). For this study, although a different analytical strategy was employed each year, for quality control purposes data can be classified as 'total' and ‘near-total’ (XRF, lithium borate fusion and multi-acid), and 'partial' (*aqua regia*). Most elements and oxides were determined twice and analysis by three different methods are available for many elements. Supported by cumulative probability plots (e.g. Fig.7) and the TILL-4 data (Appendix 4), XF, LF, and MA data for oxides can be grouped because results are similar, however AQ (Bureau Veritas *aqua regia*) data cannot be included with MA data or XF and LF data, as AQ is ‘partial’ for most elements.

Cumulative probability plots in Figure 7 illustrate differences between Na and Al from 2017 and 2018 from the three types of analyses. The shift between AQ (*aqua regia*; blue triangles) and MA (four-acid; black squares) reflects the different amounts of Al and Na liberated by the two acid-mixture dissolutions. The similar effectiveness of the XF (‘total’ XRF; red diamonds) and multi-acid methods in liberating Al and Na is shown by a general overlap of the two cumulative probability plots.

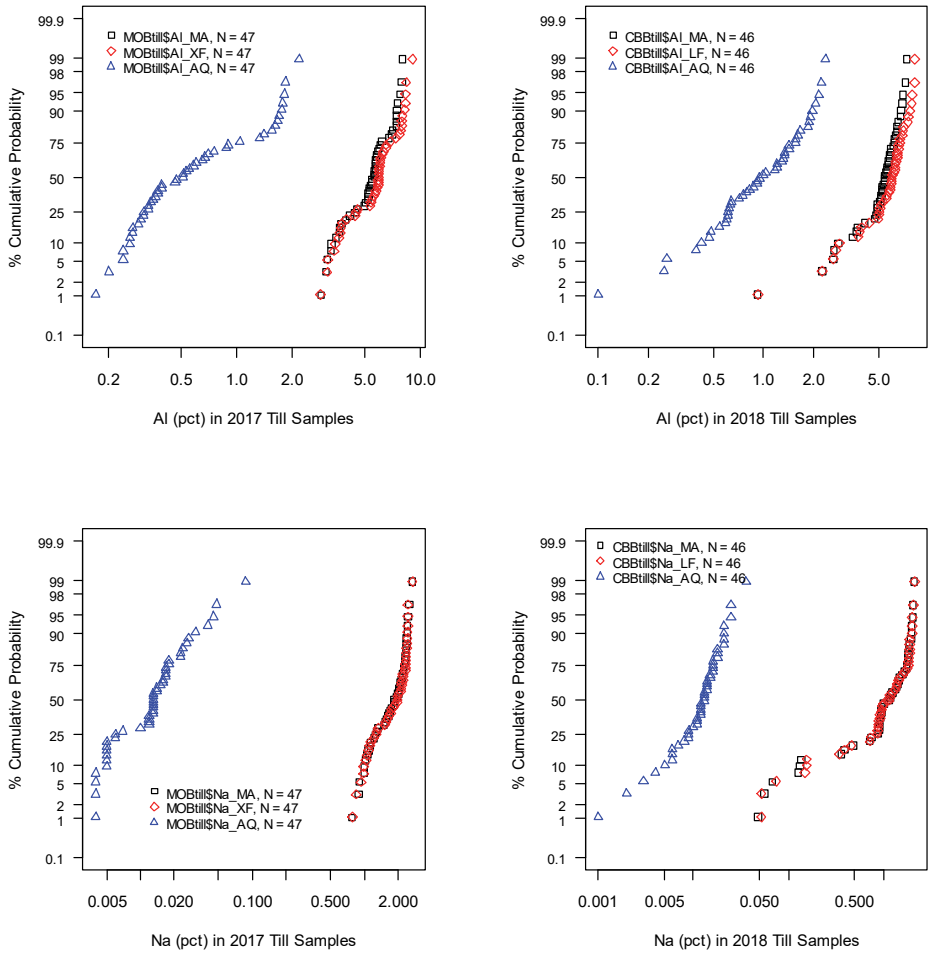

Figure 7. Cumulative probability plots for Al and Na (pct) determined in the <63 µm fraction of tills by aqua regia (Al_AQ, Na_AQ), multi-acid (Al_MA, Na_MA), X-ray fluorescence (2017samples; Al_XF, Na_XF) and Li-metaborate (2018 samples; Al_LF, Na_LF) procedures.

Blanks

Metasilicic Acid, n-Hydrate, H_20_3Si ($SiO_2.nH_20$), is a hydrated form of silicon dioxide. Aliquots of this certified lab reagent are inserted into the sample suites at approximately one per 20 analyses. Tables of mean values derived from unpublished previous analyses list elemental values obtained from each of the analytical methods used in this study, and a comparison made with the values from this study (Appendix Quality Control, Tables A4a-7 to -9). Certified Assay values include SiO_2 (min 84%), LOI as H_2O (max 16%), heavy metals as Pb (max 0.002%), sulfate (max 0.02%), non-volatiles with HF (max 0.2%), and Fe (max 0.007%).

As there are no published analytical values for individual elements, oxides or components other than SiO_2 and LOI for this reagent, it is not possible to establish whether detectable concentrations are the result of the presence of the elements in the reagent, or introduced in some part of the analytical methodology. What can be stated is that concentrations determined in the aliquots of silicic acid inserted into sample suites from 2017 and 2018 fall with two standard deviations of mean concentrations determined

from previous unpublished data, and that no significant contamination of samples in this study is apparent (Table 2).

	Trace (<0.1%)	Minor (>0.1 % <1%)	Major (>1%)
Aqua regia	Na, Ca, Sr, Sc, Ti, Cr, Cu, Zn, Zr, Mo, Hf, W, Au		
XRF/Li-borate fusion	Na_2O, MgO, CaO, Sr, Ba, Zr, Nb, Hf, Ta, W, La, Ce		SiO_2, LOI, SO_3
Multi-acid	Na, Ca, Ti, Cu, Zn, Zr, Nb, Hf, W, Pb, As, Sb, Se, Sc, Ce		

Table 2. Elements, oxides and components detected in aliquots of silicic acid at levels greater than the detection limit by three analytical methods used at the GSC (unpublished data).

Matrix colour and texture

Munsell colour codes were determined on dry samples in the GSC Sedimentology Laboratory using the SP64 Series X-Rite spectrometer. Approximately 250 g of each till sample was dry-sieved to obtain the < 2 mm fraction for till matrix texture analysis. The sand grain-size classes fractions > 0.063 mm were determined through wet-sieving (to obtain the >45 um to <2 mm size fraction) followed by dynamic image processing using a CAMSIZER Particle Size Analysis System. The classes of sizes < 0.063 mm are determined using a Lecotrac LT-100 Particle Size Analyser. Combining results from two different methods of analysis (digital imaging and laser diffraction), as well as using different subsamples, introduces a discrepancy at 0.063 mm even though there is some overlap. This should be considered when interpreting the results. The colour codes and textural data for the <2 mm fraction; sand (2-0.-063 mm), silt (0.063-0.002 mm) and clay (<0.002 mm) fractions are presented in Appendix 5. The completed grain-size and replicates data as well as ternary plots of the sand-silt-clay components are provided in Appendix 5.

Matrix carbon, organic and carbonate contents

For samples from both years, total carbon and LOI were determined on the <0.063 mm fraction at the GSC Sedimentology Laboratory. The total carbon was determined with a LECO CR-412 Carbon Analyzer instrument (1350°C; Girard et al. 2004). Only the samples with total C > 0.10% were analyzed for inorganic and organic carbon afterwards. The LOI, which is an approximation of total organic content, was determined on the <0.063 mm fraction after heating a small portion at 500°C for one hour in an ashing furnace (Girard et al., 2004). Laboratory duplicates as well as in-house (12% standard) and CANMET (Till-2, Till-4) standards were inserted for the till matrix carbon and LOI analysis. All results for the carbon and LOI analyses are given in Appendix 6.

About 1g of the <0.063 mm fraction of each of the 2017 samples was analysed to determine the calcite and dolomite content. The analysis was done using the CM Coulometer/Acid evolution method, at the GSC's Sedimentology laboratory**.** The results for the calcite and dolomite contents are provided in Appendix 6.

Clay mineralogy

The mineralogy of the clay-size fraction (separated by centrifuge at the GSC) of selected 2017 samples was determined by X-ray powder diffraction analysis (XRD) at the GSC. Mineral identification and quantitative analysis were made using EVA (Bruker AXS Inc.) software with comparison to reference mineral patterns and TOPAS (Bruker AXS Inc.), a PC-based program that performs Rietveld refinement of XRD spectra. Detailed methods and results are provided in Appendix 7.

Clast lithology

Clast lithology identification and counts were performed on the 8-30 mm size fraction of the till samples. This clast fraction was obtained by wet sieving the >2.0 mm material from the large till samples. The pebble fraction was also obtained from several small geochemistry samples where a large sample was not taken. After further screening to >8.0 mm, the pebbles were placed in an oxalic acid bath to remove the staining and residue due to weathering and oxidation. Pebbles were visually examined using a binocular microscope by P.-M. Godbout in 2017 (min 37 clasts; max 359; average 198 clasts) and by ODM in 2018 (min 34 clasts; max limit 200 clasts; average 190 clasts).

The 2017 pebble classes were grouped into the following four general lithological categories and counted by classes: a) Archean plutonic and high-grade metamorphic rocks (classes: 1-Undeformed granitic rocks, 2-Granitic rocks and orthogneiss, 3-Paragneiss, metapelite, quartzite, 4-Metagabbro/ Amphibolite 5-Quartz vein); b) Greenstones (6-Undifferentiated sediments and volcanics); c) Unmetamorphosed Proterozoic rocks (7-Thelon (Formation) quartz sandstone, 8-Pitz (Formation) Volcanics, 9-Christopher Island Formation (CIF) rhyolite, 10-Amarook sandstone) and d) Other. The 2018 pebble lithologies were separated in six groups : a) Plutonic Rocks and High Grade Metamorphic rocks (classes:1-Undeformed granitoids, 2-Granitoid gneiss and orthogneiss, 3-Paragneiss and paramigmatite, 4-Metapelite-psammite/quartzite, 5-Metachert & iron formation, 6-Meta-gabbro, 7-Amphibolite); b) Veins and tectonites (8-Quartz vein, 9-Shear zone, mylonite); c) Greenstones d) Unmetamorphosed Proterozoic rocks (10-Thelon Formation sandstone, 11-Baker Lake/Amarook sandstone, 12-Rhyolite/Syenite, 13-Pitz (Formation) volcanics, 14-Lookout Point (Formation) dolomitic sediments , 15-Diabase) and e) Other.

Review of the pebble classifications revealed limitations in the subdivisions of several of the rock types. In 2017, supracrustal clasts were grouped and classified as undifferentiated Greenstones. In 2018 the Greenstones were subdivided into rhyolites, mafic volcanics (basalt) and sediments (Greywackes) in the numbers column on the "Results 18CBB" Excel spreadsheet in Appendix 8. Review of the Greenstone counts revealed that for some samples a percentage of intermediate and mafic volcanic clasts were misclassified as greywackes (e.g. 18CBB-C009A01). It is recommended to consider the 2018 Greenstone group as undivided. Review of the count photographs may allow for further subdivision (Appendix 8). For both 2017 and 2018 counts, it was difficult to differentiate between Baker Lake Grp/Amarook Formation and Thelon Formation sandstones. As a result, it is suggested to combine the sandstone classes under a broader class - Dubawnt sandstones.

Results presented in Appendix 8 include the number of clasts in each class and the percentage (%) of the total for each class. Photographs of the classified pebbles in each sample are provided in Appendix 8 for reference (Appendix08_Till Pebble Counts\Pebble count photos).

Heavy mineral processing, Au grains and indicator mineral picking

The large till samples were processed at ODM for recovery of the heavy mineral fraction and indicator mineral counting, including gold and platinum group metals (PGM) grains, following Plouffe et al. (2013a, b) protocols and consistent with McMartin et al. (2019) and Campbell et al. (2020). Samples were processed in two separate batches and years (2017 and 2018 samples): 2017 samples in numerical order and 2018 in specified process order. The 2018 sample numbers and corresponding results are presented numerically in the Excel spreadsheets (Appendix 9).

Figure 6 summarizes the sample processing flow for the recovery of indicator minerals and precious metals grains. Samples were disaggregated and sieved to obtain the <2 mm (matrix) fraction ("Table feed"), and then, processed using a double-run across a shaking table to ensure complete recovery of all indicator minerals. The table preconcentrates were then panned for gold grains, PGMs and fine-grained metallic indicator minerals. After counting the grains, the Au grains were stored separately in a vial and any other metals minerals returned to the table concentrate. Following tabling and panning, the preconcentrates were further refined using heavy liquid (methylene iodide diluted to specifc gravity 3.2) and ferromagnetic (FM) separations using a hand magnet to produce non-ferromagnetic heavy mineral concentrates (NFM-HMC). Ferromagnetic fractions were retained and stored at the GSC. The <2 mm NFM-HMC were screened at 0.25 mm. The total number of gold, sulphide and PGM grains recovered from the panning, and the weights of the original sample, table feed, table preconcentrates, NFM- and FM-HMCs are presented in Appendix 9.

In preparation for the indicator mineral (IM) examination and selection, the 0.25-2 mm NFM-HMCs were dry sieved to 0.25-0.5 mm, 0.5-1 mm and 1-2 mm. The 0.25-0.5 mm fraction was further refined using a Carpco® electromagnetic separator to produce fractions with different paramagnetic characteristics to help reduce the volume of concentrate to be visually examined (Averill and Huneault, 2006). All fractions were examined under a stereoscopic microscope at ODM to determine the abundance of potential kimberlite indicator minerals (KIMs) and metamorphosed or magmatic massive sulphide indicator minerals (MMSIMs), and any other mineral indicating the presence of potential mineralization. For each sample, the entire concentrate in each of the three size fractions was examined. ODM performed checks on selected grains using a scanning electron microscope (SEM)-energy dispersive X-ray spectrometer (EDS) to confirm mineral identification. The 0.25-2 mm fraction were examined for scheelite grains using an ultraviolet lamp. Possible KIM and MMSIM grains were removed from the concentrates and stored in vials for further analysis. Due to the abundance of some minerals in a select number of samples, only a representative number of grains (20-50 max) were picked. All raw grain counts from the visual identification of possible indicator minerals for the 0.25-2 mm NFM-HMCs in worksheets "PGMs", "KIM Counts" and "MMSIM" for both years are also included in Appendix 9. A summary of the 2018 MMSIM counts is presented in worksheet "MMSIM Summary" in Appendix 9.

QA/QC

Two blank sand and gravel samples consisting of weathered Silurian-Devonian granite (grus; i.e. Plouffe et al., 2013a, b) were inserted by the GSC at the beginning and in the middle of each sample batch (2017 and 2018) to monitor potential cross-contamination introduced during heavy mineral separation. Data for the blank samples are listed in Appendix 9 and are highlighted in pink. Expected hornblende/titanite-zircon assemblages with no specific indicator minerals were found in the blanks. No gold, sulphides, PGMs, KIMs or MMSIMs were found in the blank samples.

A comparison of the gold grain abundance between the original and the field duplicate samples

indicates that gold grain counts are not always reproducible within the field site, likely due to the "nugget" effect. The variability is greatest for site 17MOB-056 where the gold grain counts were 28 (17MOB-056A01) and 5 (17MOB-056A02) grains respectively. For the 2018 samples, 1 field duplicate site, 18CBB-C034A01 and 18CBB-C034A02, showed some variability, 12 versus 6 gold grains, while the other field duplicate site (18CBB-C068A01 and 18CBB-C068A02)) and the lab duplicate 18CBB-C011A01and 18CBB0C011A02 had comparable gold grain results. The 2017 and 2018 field duplicates returned comparable PGMs and KIMs grain counts. The 2017 duplicates 17MOB-056A01 and17MOB-056A02 show disparities in MMSIMs grains: 1 chalcopyrite and 1 spinel in the original sample (17MOB-056A01) versus none in the field duplicate; 4 red rutile versus 1 in the duplicate, 1 epidote versus 2, 2 topaz and 3 low-Cr-diopside in the duplicate versus none in the original sample. The 2018 field duplicates have similar MMSIMS except for the following minor differences: for 18CBB-C034A01 and 18CBB-C034A02 - 10 versus 3 goethite grains, 0 versus 1 colourless spinel, 1 grain loellingite versus 1 scheelite, ~30 versus 10 red rutile grains, ~30 versus ~120 grains sillimanite and ~1500 versus ~100 orthopyroxene. Samples 18CBB-C068A01 and 18CBB-C068A02 are more similar with18CBB-C068A01 having 1 scheelite grain, 1 red rutile grain versus none in the duplicate (18CBB-C068A02), as well as less kyanite, apatite, staurolite and orthopyroxene grains than 18CBB-C068A02. The lab duplicate samples, 18CBB-C011A01/A02 show similar MMSIM mineralogy. All picking results for the lab duplicate (grey), blanks (pink) and the field duplicate (yellow) samples are reported in Appendix 9. The metadata for the indicator mineral processing and picking work is summarized in Appendix 11.

Scanning electron microscope quantitative analysis

Selected potential indicator minerals from the 0.25-0.50 mm and 0.5-1.0 mm fractions were sent to IOS Services Géoscientifiques inc. for grain mounting and probe work (2017 samples: n=108 grains; 2018 samples: n=101 grains). The grains were mounted on epoxy stubs and polished (0.05 μm depth). A sputter coater with a palladium target was used to metalize the surface of the mount. The metal coating thickness is ~10 nm. The following minerals were mounted: 2017 samples - chromite, epidote, forsterite, grossular, low-Cr diopside, Mn-epidote, sapphirine, sillimanite, spessartine and spinel; 2018 samples - almandine, blue spinel, chromite, florencite, gahnite, hercynite, low-Cr diopside, sapphirine, spinel and topaz.

Grains were analysed with a 2013 Zeiss EVO MA 15-HD SEM. The microscope is equipped with a high sensibility Oxford Instruments X-Max 150 EDS-SDD detector, a CZBSD sector backscattered electron detectors, two secondary electron detectors and a cathodoluminescence detector. A LaB6 filament was used at its second saturation point in order to ensure the stability of the electron beam. Quantitative analyses were performed under vacuum at 20 kV, with an aperture of 60 μm (high current), specimen current of 3.17 nA. In order to quantify minor elements, acquisition count was set at two million counts per spectrum, divided into 2048 channels. Backscatter election imaging was used for the selection of the analysis sites on the minerals. A more detailed description of the SEM quantitative analysis and quality control data, including calibration, are provided in the IOS reports (Appendix 10). The analysed grains were classified on the basis of their chemical composition and the data by mineral species (pyroxene, spinel, olivine, epidote, REE, sulfides and others). Analytical results are provided in the IOS reports and in Excel files in Appendix 10. The metadata for the quantitative SEM work is summarized in Appendix 11.

SUMMARY

The Geological Survey of Canada completed targeted till sampling surveys in 2017 in eastern Keewatin (Sector 1) and in 2018 in western Keewatin (Sector 2), mainland Nunavut and eastern Northwest Territories in partnership with the Canada-Nunavut Geoscience Office (CNGO) and the Northwest Territories Geological Survey (NTGS). These survey were part of Natural Resources Canada's GEM-2 Rae Synthesis of Glacial History and Dynamics Activity. The field and analytical methods and the analytical results for both surveys are provided in this report. Quaternary field observations were recorded at 164 field stations (2017- n=92; 2018 – n=72) which included small-scale ice-flow indicator measurements at 74 sites (2017 - n= 34 sites; 2018 – n=40 sites). Surface till samples were collected at 82 locations from a variety of glacial terrains during both field seasons – either in targeted areas or along transects. Five transects were sampled to document glacial transport both within ice streams (e.g. DLIS), over the KID in eastern Keewatin and across paleoglaciological domains such as in western Keewatin (e.g. DLIS - warm-based - relict- palimpsest terrains). The transects were designed to follow and test various ice-flow phases. Geochronology sampling included 27 bedrock or boulder samples for TCN dating and 5 sand samples for ISRL dating. The methodology and results for the age dating will form the basis of a subsequent publication.

Analytical results include till matrix texture, colour, carbon, carbonate and organic contents, clast lithology, as well as results from till matrix geochemistry and indicator mineral picking and SEM analysis. The till matrix geochemical analyses were performed on the <0.063 mm fraction using ICP-MS modified *aqua regia* digestion, ICP-MS 4-acid digestion, and ICP-ES/MS lithium borate fusion and for 2017 samples XRF analysis. Heavy mineral processing, precious metal grain counts, indicator mineral identification and picking were completed for each large till sample. The mineralogy of selected indicator mineral grains was determined using quantitative SEM. The QA/QC analyses using field and analytical duplicates as well as control reference samples (blanks and standards) were also evaluated. The analytical and QA/QC procedures follow the protocols for till samples collected as part of GEM projects (McClenaghan et al., 2020; Plouffe et al., 2013a). All the field datasets and the complete analytical results are presented in Excel spreadsheet format.

ACKNOWLEDGEMENTS

This work was conducted as part of Glacial History and Dynamics Activity within the GEM-2 Rae Project. The 2017 field project in Nunavut was a collaboration with the Western Hudson Bay Project (T. Tremblay, CNGO), and partly funded by Strategic Investments in Northern Economic Development (SINED) in partnership with the Canada-Nunavut Geoscience Office. We gratefully acknowledge Helen Moffat and Boris Kotelewetz in Baker Lake, and Theresa Blacquiere and Don St-John in Arviat, for their lodging and expediting services, Ookpik Aviation and Prairie Helicopters (Doug Potts) for fixed and rotary wing support respectively, and Polar Continental Shelf Program for logistical support (Project # 056-17). Shania Tookoome of Baker Lake and Justin Suluk of Arviat are thanked for their enthusiastic assistance in the field.

The 2018 component of this project was a collaboration with the Northwest Territories Geological Survey (P. Normandeau, Northwest Territories Geological Survey Contribution #0142) and partly funded by Strategic Investments in Northern Economic Development (SINED). We are grateful for the opportunity to base our field operation out of Aylmer Lake Lodge and wish to thank our host Kevin and Patti McNeil for their hospitality and support. Summit Air (Fixed wing) and Summit Helicopters (Paula Vera) capably provided air support. Logistical support was provided by Polar Continental Shelf Program (Project #064-18).

We are most appreciative of Louis Robertson, Aeron Vaillancourt, Sabrina Chan, Sarah Mount, Guy Buller, and Étienne Girard for the GIS support before, during and after the fieldwork. Special thanks to Charles Fortin and Charles Papasodoro from the Canada Centre for Mapping and Earth Observation in Sherbrooke (QC) for providing the ArcticDEM datasets. The authors also give special thanks to Iyse Randour for her work compiling the datasets in the appendices. Finally, we thank Dan Kerr (GSC), Natasha Wodicka (GSC), Holly Steenkamp (CNGO), Daniel Sincennes, Rosie Khoun and Kate Clark (GEM Office), Geneviève Marquis (GSC), Linda Ham (CNGO), and Scott Cairns (NTGS) for enthusiastic support for the project and assistance prior to and during the fieldwork. We thank Jessey Rice for the internal review the report.

REFERENCES

Averill, S. and Huneault, R., 2006. Overburden Drilling Management Ltd: Exploring heavy minerals; EXPLORE, Newsletter of the Association of Applied Geochemists, v. 133, p. 1–5.

Aylsworth, J.M. and Shilts, W.W., 1989. Glacial features around the Keewatin Ice divide: Districts of MacKenzie and Keewatin; Geological Survey of Canada, Paper 88-24, 21 p.

Bateman, M.D., 2015. The Application of luminescence dating in sea-level studies. In: Shennan I, Long, A.L. and Horton, B.P. (Eds), Handbook of Sea-Level Research, Wiley-Blackwell, Chapter 27.

Behnia, P., McMartin, I., Campbell, J.E., Godbout, P.-M., and Tremblay, T., 2020. Northern Canada glacial geomorphology database 2020: Part 1 – Central Mainland Nunavut. Geological Survey of Canada, Open File 8717, 8 p., 5 tables, 2 maps and geodatabase.

Bureau Veritas Minerals, 2021. Geochemistry: schedule of services & fees (CAD), 48 p.

Burnham, O.M. and Schweyer, J., 2004. Trace element analysis of geological samples by inductively coupled plasma mass spectrometry at the Geoscience Laboratories: revised capabilities due to improvements to instrumentation in Summary of Field Work and Other Activities 2004; Ontario Geological Survey, Open File Report 6145, p. 54-1 to 54-20.

Campbell, J.E., Lauzon, G., Dyke, A. and Haiblen, A.M., 2016. Report of 2016 Activities for the Regional Surficial Geological Mapping of the South Rae Craton, Southeast NWT: GEM 2 South Rae Quaternary and Bedrock Project; Geological Survey of Canada, Open File 8143, 13 p.

Campbell, J.E., Lauzon, G., Dyke, A.S. and Roy, M., 2017. Regional glacial history, paleo-dynamics and dispersal patterns, South Rae craton, Northwest Territories; Kingston 2017; Geological Association of Canada-Mineralogical Association of Canada, Kingston, Ontario, Program with abstracts, v. 40, p. 48.

Campbell, J.E., McMartin, I, Normandeau, P.X., and Godbout, P.-M., 2019. Report of 2018 activities for the GEM-2 Rae project glacial history activity in the eastern Northwest Territories and the Kitikmeot and Kivalliq Regions, Nunavut; Geological Survey of Canada, Open File 8586, 18 p. https://doi.org/10.4095/314741

Campbell, J.E., McCurdy, M.W., Lauzon, G., Regis, D. and Wygergangs, M., 2020. Field data, till composition and ice-flow history, south Rae craton, NWT: results from the GEM2 South Rae project - Surficial Mapping activity; Geological Survey of Canada, Open File 8714, 40 p., https://doi.org/10.4095/327218.

Craig, B.G., 1964. Surficial geology of the east-central district of Mackenzie; Geological Survey of Canada Bulletin 99, 41 p., 2 maps.

Crock, J.G. and Lamothe, P.J., 2011. Inorganic chemical analysis of environmental materials – A lecture series: U.S Geological Survey Open-File Report 2011-1193, 117 p.

Dalton, A. S., Margold, M., Stokes, C. R., Tarasov, L., Dyke, A. S. et al., 2020. An updated ice margin chronology for the North American Ice Sheet Complex. Quaternary Science Reviews, v. 234, Article 106223. 10.1016/j.quascirev.2020.106223

Fletcher, W.K., 1981. Analytical methods in geochemical prospecting. In: Govett, G.J.S. (Ed.), Handbook of Exploration Geochemistry, Vol. 1; Analytical Methods in Geochemical Prospecting. Elsevier, Amsterdam, 255 p.

Girard, I., Klassen, R.A. and Laframboise, R.R., 2004: Sedimentology Laboratory Manual, Terrain Sciences Division; Geological Survey of Canada, Open File 4823, 134 p.

Gosse, J.C. and Phillips, F.M., 2001. Terrestrial in suite cosmogenic nuclides: theory and application; Quaternary Science Reviews, v. 20, p.1475-1560.

Harrison, J.C., St-Onge, M.R., Petrov, O.V., Strelnikov, S.I., Lopatin, B.G., Wilson, F.H., Tella, S., Paul, D., Lynds, T., Shokalsky, S.P., Hults, C.K., Bergman, S., Jepsen, H.F. and Solli, A., 2011. Geological map of the Arctic / Carte géologique de l'Arctique; Geological Survey of Canada, Map 2159A, scale 1:5 000 000.

Huntley, D.J. and Lian, O.B. 1999. Using optical dating to determine when a sediment was last exposed to sunlight. In Holocene climate and environmental change in the Palliser Triangle: a geoscientific context for evaluation the impacts of climate change on the southern Canadian prairies; D.S. Lemmen and R.E.Vance (ed). Geological Survey of Canada, Bulletin 534, pp. 211–222.

Kjarsgaard, B. A., Plourde, A.P., Knight, R. D., and Sharpe, D. R., 2014. Geochemistry of regional surficial sediment samples from the Thelon River to the East Arm of Great Slave Lake, Northwest Territories, Canada; Geological Survey of Canada, Open File 7649; 17 p, doi:10.4095/295195.

Lamothe, M., 2016. Luminescence dating of interglacial coastal depositional systems: Recent developments and future avenues of research; Quaternary Science Reviews, v. 146 (Supplement C), p. 1-27.

Lynch, J.J., 1996. Provisional elemental values for four new geochemical soil and till reference materials, TILL-1, TILL-2, TILL-3 and TILL-4; Geostandards Newsletter, v. 20, no. 2, p. 277-287.

McClenaghan, M. B., Spirito, W. A., Plouffe, A., McMartin, I., Campbell, J. E., Paulen, R. C., Garrett, R. G., Hall, G. E. M., Pelchat, P., and Gauthier, M. S., 2020. Geological Survey of Canada till-sampling and analytical protocols: from field to archive, 2020 update; Geological Survey of Canada, Open File 8591, 73 p. https://doi.org/10.4095/326162

McCurdy, M.W., and Garrett, R.G., 2016. Geochemical Data Quality Control for Soil, Till and Lake and Stream Sediment Samples; Geological Survey of Canada, Open File 7944, 35 p.

McMartin, I., 2017. Till provenance across the terminus of the Dubawnt Lake Ice Stream, central Nunavut; Geological Survey of Canada, Current Research 2017-1, 13 p.

McMartin, I. 2000. Till composition across the Meliadine Trend, Rankin Inlet area, Kivalliq region, Nunavut; Geological Survey of Canada, Open File 3747, 330 p. 1 CD-ROM, https://doi.org/10.4095/211793

McMartin, I., Berman, R.G., Normandeau, P.X., and Percival, J.A., 2013. Till composition of a transect across the Thelon tectonic zone, Queen Maud block, and adjacent Rae craton: results from the Geo-Mapping Frontiers' Chantrey project; Geological Survey of Canada, Open File 7418, 22 p.

McMartin, I., Campbell, J.E., Dredge, L.A., LeCheminant, A.N., McCurdy, M.W. and Scromeda, N., 2015. Quaternary geology and till composition north of Wager Bay, Nunavut: results from the GEM Wager Bay Surficial Geology Project; Geological Survey of Canada, Open File 7748, 53 p.

McMartin, I., Tremblay, T. and Godbout, P.-M., 2017. Report of 2017 field activities for the GEM-2 Rae glacial history activity in the Kivalliq region, Nunavut; Geological Survey of Canada, Open File 8320, 14 p. https://doi.org/10.4095/306006

McMartin, I., Randour, I. and Wodicka, N., 2019. Till composition across the Keewatin Ice Divide in the Tehery-Wager GEM-2 Rae project area, Nunavut; Geological Survey of Canada, Open File 8563, 1 .zip file. https://doi.org/10.4095/314707

McMartin, I., Godbout, P.-M., Campbell, J.E., Tremblay, T. and Behnia, P., 2020. A new map of glacigenic features and glacial landsystems in central mainland Nunavut, Canada; Boreas, v. 50. p. 51-75. https://doi.org/10.1111/bor.12479

Paul, D., Hanmer, S., Tella, S., Peterson, T.D. and LeCheminant, A.N., 2002. Compilation, bedrock geology of part of the western Churchill Province, Nunavut - Northwest Territories; Geological Survey of Canada, Open File 4236, Scale 1:1 000 000 map.

Plouffe, A., McClenaghan, M.B., Paulen, R.C., McMartin, I., Campbell, J. and Spirito, W., 2013a. Processing of unconsolidated glacial sediments for the recovery of indicator minerals: protocols used at the Geological Survey of Canada; Geochemistry, Exploration, Environment, Analysis, v. 13, p. 303-316.

Plouffe, A., McClenaghan, M.B., Paulen, R.C., McMartin, I., Campbell, J.E. and Spirito, W.A., 2013b. Quality assurance and quality control measures applied to indicator mineral studies at the Geological Survey of Canada; in Paulen, R.C. and McClenaghan, M.B. (eds.), New Frontiers for Exploration in Glaciated Terrain, Geological Survey of Canada, Open File Report 7374, p. 13-19.

Porter, C., Morin, P., Howat, I., Noh, M.-J., Bates, B., Peterman, K., Keesey, S., Schlenk, M., Gardiner, J., Tomko, K., Willis, M., Cloutier, M., Husby, E., Foga, S., Nakamura, H., Platson, M., Wethington, M. J., Williamson, C., Bauer, G., Enos, J., Arnold, G., Kramer, W., Becker, P., Doshi, A., D'souza, C., Cummens, P., Laurier, F. and Bojesen, M. 2018; ArcticDEM. Harvard Dataverse, v1. https://doi.org/10.7910/DVN/OHHUKH

Prest, V.K., Grant, D.R. and Rampton, V.N., 1968. Glacial Map of Canada; Geological Survey of Canada, Map 1253A, Scale 1:5 000 000.

Rainbird, R.H., Hadlari, T., Aspler, L.B., Donaldson, J.A., Lecheminant, A.N. and Peterson, T.D., 2003. Sequence stratigraphy and evolution of the Paleoproterozoic intracontinental Baker Lake and Thelon Basins, western Churchill Province, Nunavut; Precambrian Research, v. 125, p. 21-53.

Randour, I., McMartin, I. and Roy, M., 2016. A study of the postglacial marine limit between Wager Bay and Chesterfield Inlet, Nunavut; in Summary of Activities 2016, Canada-Nunavut Geoscience Office, p. 51-60.

Staiger, J.W., Gosse, J., Little, E.C., Utting, D.J., Finkel, R., Johnson, J.V. and Fastook, J., 2006. Glacial erosion and sediment dispersion from detrital cosmogenic nuclide analyses of till; Quaternary Geochronology, v. 1, p. 29-42.

Thompson, M. and Howarth, R.J., 1973. The rapid estimation and control of precision by duplicate determinations; The Analyst, v. 98, p. 153-160.